


Progressive evolution of whole-rock composition during metamorphism revealed by multivariate statistical analyses

Kenta Yoshida¹  | Tatsu Kuwatani^{1,2} | Takao Hirajima³ | Hikaru Iwamori¹ | Shotaro Akaho⁴

¹Japan Agency for Marine-Earth Sciences and Technology, Yokosuka, Japan

²PRESTO, Japan Science and Technology Agency (JST), Kawaguchi, Japan

³Department of Geology and Mineralogy, Kyoto University, Kitashirakawa-Oiwakecho, Kyoto, Japan

⁴National Institute of Advanced Industrial Science and Technology, Tsukuba, Ibaraki, Japan

Correspondence

Kenta Yoshida, Japan Agency for Marine-Earth Sciences and Technology, Yokosuka, Kanagawa, Japan.
Email: yoshida_ken@jamstec.go.jp

Funding information

Japan Society for the Promotion of Science, Grant/Award Number: 15K20864, 16K17835, 25120011, 2512005, 25257208; Precursory Research for Embryonic Science and Technology, Grant/Award Number: JPMJPR1676

Handling Editor: Katy Evans

ABSTRACT

The geochemical evolution of metamorphic rocks during subduction-related metamorphism is described on the basis of multivariate statistical analyses. The studied data set comprises a series of mapped metamorphic rocks collected from the Sanbagawa metamorphic belt in central Shikoku, Japan, where metamorphic conditions range from the pumpellyite–actinolite to epidote–amphibolite facies. Recent progress in computational and information science provides a number of algorithms capable of revealing structures in large data sets. This study applies *k*-means cluster analysis (KCA) and non-negative matrix factorization (NMF) to a series of metapelites, which is the main lithotype of the Sanbagawa metamorphic belt. KCA describes the structures of the high-dimensional data, while NMF provides end-member decomposition which can be useful for evaluating the spatial distribution of continuous compositional trends. The analysed data set, derived from previously published work, contains 296 samples for which 14 elements (Si, Ti, Al, Fe, Mn, Mg, Ca, Na, K, P, Rb, Sr, Zr and Ba) have been analysed. The KCA and NMF analyses indicate five clusters and four end-members, respectively, successfully explaining compositional variations within the data set. KCA indicates that the chemical compositions of metapelite samples from the western (Besshi) part of the sampled area differ significantly from those in the east (Asemigawa). In the west, clusters show a good correlation with the metamorphic grade. With increasing metamorphic grade, there are decreases in SiO₂ and Na₂O and increases in other components. However, the compositional change with metamorphic grade is less obvious in the eastern area. End-member decomposition using NMF revealed that the evolutionary change of whole-rock composition, as correlated with metamorphic grade, approximates a stoichiometric increase of a garnet-like component in the whole-rock composition, possibly due to the precipitation of garnet and effusion of other components during progressive dehydration. Thermodynamic modelling of the evolution of the whole-rock composition yielded the following results: (1) the whole-rock composition at lower metamorphic grade favours the preferential crystallization of garnet under the conditions of the garnet zone, with biotite becoming stable together with garnet in higher-grade

rock compositions under the same P – T conditions; (2) with higher-grade whole-rock compositions, more H_2O is retained. These results provide insight into the mechanism suppressing dehydration under high- P metamorphic conditions. This mechanism should be considered in forward modelling of the fluid cycle in subduction zones, although such a quantitative model has yet to be developed.

KEYWORDS

material cycle, multivariate statistical analysis, pseudosection analysis, Sanbagawa metamorphism, subduction zone

1 | INTRODUCTION

The geochemical evolution of metamorphic rocks in subduction zones has been a topic of intense research for the last quarter century (e.g. Bebout, Ryan, & Leeman, 1993; Konrad-Schmolke, O'Brien, & Zack, 2011; White, Powell, & Holland, 2001). Thermodynamic calculations can predict the evolution of mineral assemblages under a wide range of P – T conditions for specific whole-rock compositions; that is, pseudosection modelling (Connolly, 2005; Holland & Powell, 1998). Most previous studies dealing with pseudosection analysis have been based on a foursquare assumption that major components of whole-rock composition have constant ratios, except for a few studies considering mineral fractionation or melt loss (Evans, 2004; Tinkham & Ghent, 2005; White et al., 2001). Evans (2004) discussed the “effective” bulk composition derived from garnet crystal fractionation and its effect on isopleth geothermobarometry. In this context, the effective bulk composition mainly involves the fractionation of zoned minerals, while the actual whole-rock composition is assumed to be constant. This assumption seems valid, until partial melting starts, as metamorphic reactions are modelled by solid–solid reactions, and all reacting substances, except for certain volatiles, are stored in the reaction products. Significant mass transfer including major and trace elements has been recognized along the localized fluid pathway (e.g. Higashino et al., 2015; John et al., 2012; Okudaira, Shigematsu, Harigane, & Yoshida, 2017), whereas studies on main rock bodies without such localized fluid flows yield “fluid mobile” elements such as lead are immobile up to eclogite facies (Spandler, Hermann, Arculus, & Mavrogenes, 2003). However, some recent studies have shown that even “fluid-immobile” elements (e.g. Ti) are mobile under specific conditions of metamorphic processes (Audetát & Keppler, 2005). This may indicate the modification, or evolution, of whole-rock composition during metamorphism where partial melting events has not occurred.

Generally, spatial differences in whole-rock composition are evident at scales in hand specimen, and this inhomogeneity has obstructed the evaluation of metamorphic

evolution. Recent progress in data-mining has the potential to overcome such problems by dealing with large data sets containing a number of data points with enormous dimensions (e.g. Igarashi et al., 2016). Compositional diagrams in low-dimension systems (with 2D or 3D projections) are useful for characterization and thus have been employed for a long time (e.g. Kouketsu & Enami, 2011; Thompson, 1957), but they can obscure true structures built up in the higher dimension (Iwamori et al., 2017). Appropriate multivariate statistical analyses are, therefore, required to extract the true characteristics of large, complicated data sets.

To evaluate the metamorphic evolution of whole-rock composition, a number of rock samples, with assumed “similar” composition, must be investigated over a wide range of pressures and temperatures. The Sanbagawa metamorphic belt in SW Japan consists mainly of widely exposed metapelites and is one of the most well-studied metamorphic terranes worldwide (e.g. Higashino, 1990). The mineral assemblages and P – T conditions are well constrained (e.g. Banno, 2004). There is a small number of sources providing considerable whole-rock composition data (Goto, Higashino, & Sakai, 1996; Kiminami & Ishihama, 2003). This study seeks to describe the metamorphic evolution of the metapelites under intermediate high- P/T metamorphism by means of statistical analysis and machine-learning techniques. A systematic change in whole-rock composition with the degree of metamorphism is observed, and its significance is discussed. Mineral abbreviations follow Whitney and Evans (2010).

2 | GEOLOGICAL BACKGROUND AND ANALYSED DATA SET

The Sanbagawa metamorphic belt is exposed mainly in southwest Japan (Figure 1a). Four mineral zones are recognized on the basis of the mineral assemblages of pelitic schists (from the lower to higher grade): the chlorite, garnet, albite–biotite and oligoclase–biotite zones (Figure 1b; Enami, 1982; Kurata & Banno, 1974; Higashino, 1990). Peak P – T conditions have been estimated as pumpellyite–actinolite facies (300–360°C/0.55–0.65 GPa) for the

chlorite zone to epidote–amphibolite facies (585–635°C/0.9–1.1 GPa) for the oligoclase–biotite zone (Figure 1c) (e.g. Aoya et al., 2013; Enami, Wallis, & Banno, 1994). In contrast, eclogite-facies rocks present in central and eastern Shikoku yield distinct P – T conditions of quartz–eclogite facies, indicating lower-temperature subduction (Endo, Wallis, Tsuboi, Aoya, & Uehara, 2012; Takasu, 1984; Wallis & Aoya, 2000). Furthermore, a recent study provided evidence for further cooler subduction of the lawsonite–eclogite facies (the Kotsu eclogite in eastern Shikoku; Tsuchiya & Hirajima, 2013).

There have been few studies dealing with the compositional variation of the Sanbagawa metapelites (e.g. Goto et al., 1996; Kiminami & Ishihama, 2003; Kouketsu & Enami, 2011). Kouketsu and Enami (2011) showed that metapelites in the Sanbagawa metamorphic belt have low X_{Na} values [$=\text{Na}/(\text{Na}+\text{Al}-2\text{K}-1.5)$] and attributed this to the rare occurrence of omphacite, a typical index mineral of high- P metamorphism, from eclogite-facies metapelites.

Goto et al. (1996) provided a whole-rock composition data set with a reliable sample-location map (Figure 1b), containing 195 samples with 10 major elements (Si, Ti, Al, Fe, Mn, Mg, Ca, Na, K and P) and nine trace elements (Rb, Sr, Y, Zr, Nb, Ba, Th, Pb and Ni). Kiminami and Ishihama (2003) provided whole-rock composition data together with the metamorphic grade and sampling area, but not with detailed sample locations. They reported analyses of 101 samples for similar major elements to Goto et al. (1996) and nine trace elements (Ba, Cr, Nb, Rb, Sr, V, Y, Zn and Zr). Since many statistical analyses can only be computed for complete data sets, Cr, V, Zn, Th, Pb and Ni are not included in analyses. Furthermore, Y and Nb show obvious difference between two data sets, probably because of the difference in laboratory procedure; that is, the results of Goto et al. (1996) are lower than those of Kiminami and Ishihama (2003). Therefore, these two elements were also excluded from the present analyses. Overall, a total of 296 samples with 14 elements (Si, Ti, Al, Fe,

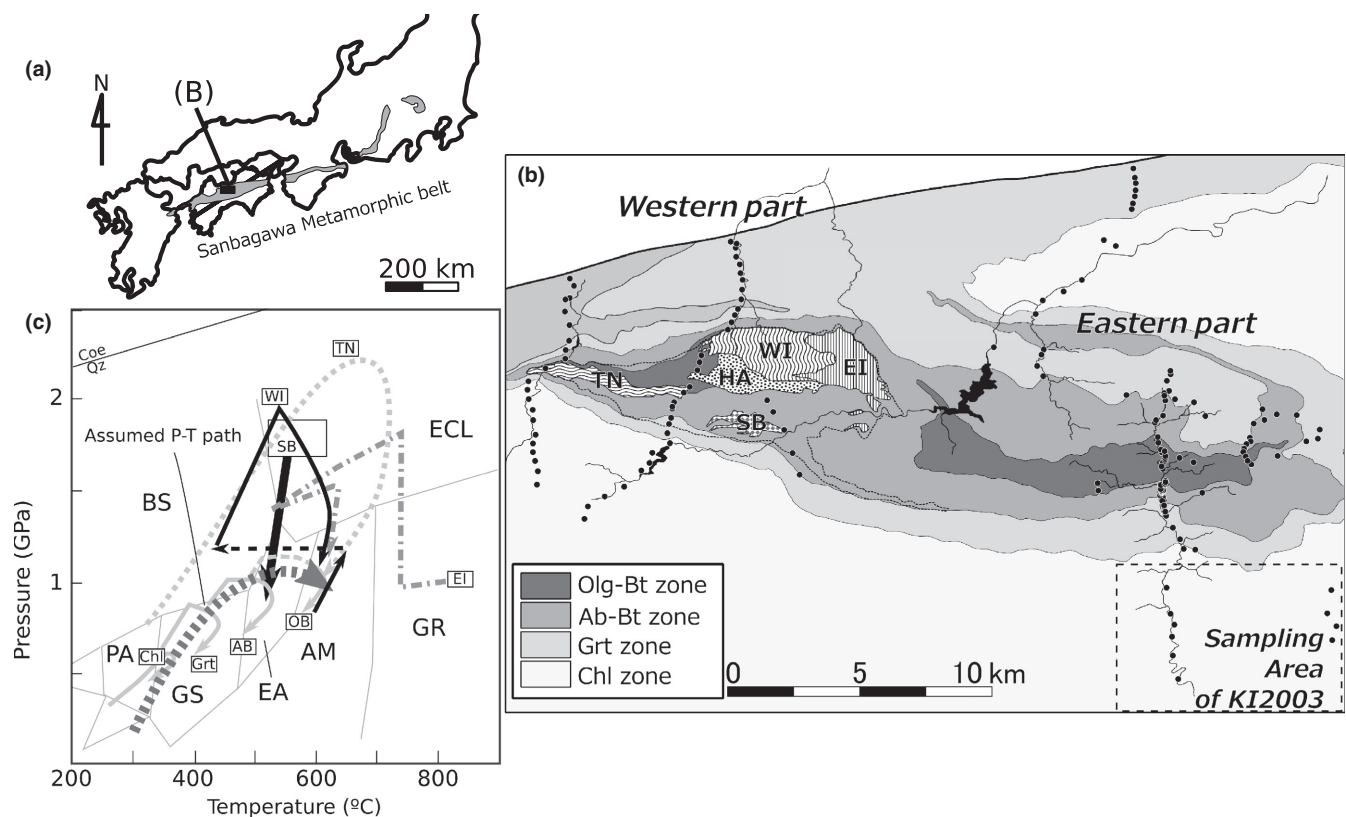


FIGURE 1 (a) Areal distribution of the Sanbagawa metamorphic belt in southwest Japan. Also shown is the location of the studied area in central Shikoku. (b) Zonal metamorphic map of the central Shikoku area after Higashino (1990) and Aoya et al. (2013). Dashed line in the western area is the suggested boundary of the eclogite nappe (Aoya et al., 2013). Sample localities from Goto et al. (1996) are also shown. Sample locality area from Kiminami and Ishihama (2003) is also shown as the dashed rectangle (KI2003). Abbreviations for eclogite bodies are as follows: WI, western Iratsu body; EI, eastern Iratsu body; HA, Higashi–Akaishi peridotite body; TN, Tonaru metagabbro body; and SB, Seba body. (c) P – T estimate based on previous publications, mainly based on the compilation of Aoya (2001) partly referring Enami et al. (1994). P – T estimation for TN and WI are after Miyagi and Takasu (2005) and Endo (2010), respectively. Assumed P – T path used the thermodynamic modelling is also shown. Abbreviations for metamorphic facies are as follows: PA, pumpellyite–actinolite facies; GS, greenschist facies; EA, epidote–amphibolite facies; AM, amphibolite facies; GR, granulite facies; BS, blueschist facies; ECL, eclogite facies

Mn, Mg, Ca, Na, K, P, Rb, Sr, Zr and Ba) were used for analysis in this study.

3 | METHODS

3.1 | Multivariate statistical analysis

Compositional variations in whole-rock chemistry over continuous or discrete bodies have been investigated by many studies, especially for igneous rocks (e.g. Batchelor & Bowden, 1985; Brandmeier & Wörner, 2016; Maier, Arndt, & Curl, 2000; Verma et al., 2017). Previous publications have focused mainly on empirically established characteristics (e.g. element ratios) and typical geochemical plots to extract compositional features. Although these well-established approaches provide reliable results, the structures of compositional data sets can be complicated and may be misinterpreted by graphical methods (Iwamori et al., 2017). To correctly and fully extract information from a high-dimensional data set, we have applied multivariate analysis to log ratio-transformed compositional data. This approach sidesteps the constant-sum constraint that precludes compositional data from much of statistical analysis (e.g. Aitchison, 1986; Ohta & Arai, 2006; Pawlowsky-Glahn & Egozcue, 2006; Tolosana-Delgado, Otero, & Pawlowsky-Glahn, 2005).

A schematic of the multivariate analyses applied in this study is shown in Figure 2. The 195 samples with

compositional data for 14 elements and detailed sample locations (Goto et al., 1996) and 101 samples without detailed sample locations (Kiminami & Ishihama, 2003) were used for multivariate analysis. These data were transformed by means of centred logratio transformation (CLR), which emphasizes relative magnitudes and variations in components rather than absolute values. Given the total number of samples as D , the i th centred logratio transformed data point z_i is calculated as follows:

$$z_i = \ln \frac{x_i}{g(\mathbf{x})} \quad (1)$$

where $g(x)$ is the geometric mean calculated, using the product symbol for the j th sample, as follows:

$$g(\mathbf{x}) = \left(\prod_j^D x_j \right)^{1/D} \quad (2)$$

Transformed data sets were then treated with further statistical analyses following Iwamori et al. (2017), who provided a classification scheme for geochemical data sets including CLR, primary standardization, whitening (sphering), principal component analysis (PCA) and k -means cluster analysis (KCA). Primary standardization is the transformation that sets the mean of variables to 0 and SD to 1. Whitening decorrelates variables and sets the variance to 1. Standardized and whitened data matrices were then treated with further statistical analysis,

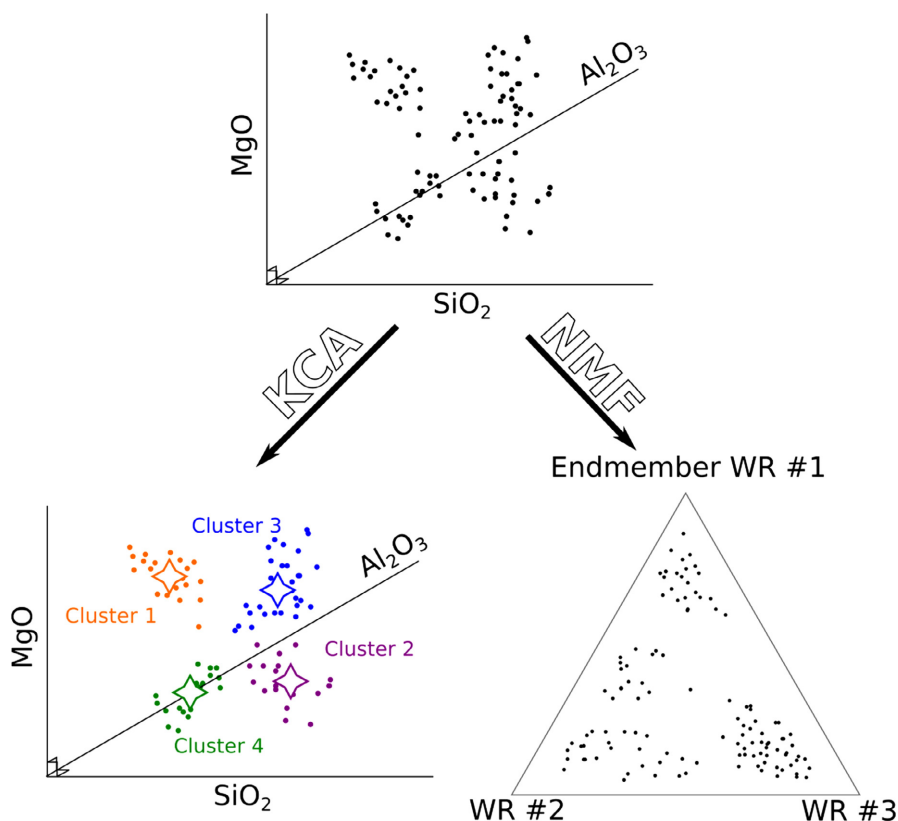


FIGURE 2 Schematic image of the multivariate analyses applied in this study. k -means cluster analysis (KCA) divides the data set into clusters by evaluating the distance between each data point. Large symbols plotted in the KCA results indicate the mean composition of each cluster; that is, centroids. NMF performs end-member decomposition, which can best explain the variation in the studied data set

such as PCA and KCA. PCA is a commonly used method for identifying the uncorrelated base vectors by maximizing the variance along the principal components (PCs). KCA is a classification method that divides multivariate data into a set of k clusters which minimize the total distance between centroids (mean of a cluster). According to Iwamori et al. (2017), KCA for the standardized and whitened data gives a discretized set of solutions equivalent to independent component analysis (ICA), while KCA for standardized (but not whitened) data is equivalent to PCA. In this study, KCA was applied to standardized and whitened data sets, which is analogous to ICA.

To specify compositional trends in analysed data, non-negative matrix factorization (NMF) was applied. NMF is a method of unsupervised machine learning which aims at decomposing an original data set into subcomponents without negative values. This decomposition transforms the original compositional data into the addition of base vectors; that is, the original composition is expressed as the mixture of “end-member” components, similar to description of solid-solution minerals.

Although NMF has many varieties of formulation (Aggarwal & Zhai, 2012), a model known as the “Topic model” was applied here because it is particularly suitable for dealing with compositional data. The Topic model was originally developed to find topics from Internet news articles based on frequencies of words included in each article. In the present context, this corresponds to finding end-members based on the frequencies of elements that make up the rock of interest. Suppose a compositional data matrix, V , whose i th row is the element ratio of the i th sample. The Topic model attempts to find a matrix decomposition as follows:

$$V \cong WH \quad (3)$$

$$\sum_j V_{ij} = 1, \sum_k W_{i,k} = 1, \sum_j H_{k,j} = 1 \quad (4)$$

where the composition of the k th end-member is represented as the k th row of H , and its mixing ratio for the i th member is represented as the i th row of W . The matrix decomposition is performed to minimize the Kullback–Leibler divergence between V and WH , which is a natural distance measure for compositional data.

In addition, Bayesian estimation is performed to stabilize the estimation by introducing Dirichlet distribution as prior distributions for W and H . This formulation of the Topic model is known as latent Dirichlet allocation (Blei, Ng, & Jordan, 2003).

By using the obtained end-member compositions, dimension reduction can be performed. In this study, we found four whole-rock composition end-members that explain the variation of the studied data set well.

3.2 | Thermodynamic modelling

On the basis of the characterization of the studied data set, thermodynamic modelling was performed to estimate the mineral parageneses observed in the field. Pseudosection modelling was performed using Perple_X 6.7.1 (Connolly, 2005) updated on 11 April 2015. Stable phase relations were examined in the $P(T)$ - X phase diagrams assuming a prograde P - T trajectory and end-member whole-rock compositions. The chemical system of $\text{MnO-Na}_2\text{O-CaO-K}_2\text{O-FeO-MgO-Al}_2\text{O}_3\text{-SiO}_2\text{-H}_2\text{O}$ was adopted with an excess of H_2O . The following solid-solution models were used for calculations: white mica (Auzanneau, Schmidt, Vielzeuf, & Connolly, 2010; Coggon & Holland, 2002), amphibole (Dale, Powell, White, Elmer, & Holland, 2005), Na-Ca-mica (Bucher-Nurminen, Frank, & Frey, 1983; Frank, 1983), ilmenite (White, Powell, Holland, & Worley, 2000), and biotite, chlorite, plagioclase, K-feldspar, garnet, and clinopyroxene (Holland & Powell, 1998).

A number of publications have reported P - T estimates of prograde and retrograde stages of the Sanbagawa metamorphic belt (e.g. Enami et al., 1994; Endo et al., 2009; Yoshida et al., 2016). Figure 1c summarizes the available P - T estimations. To construct a simple model, a prograde P - T path was assumed based on the peak P - T estimation for the chlorite to oligoclase–biotite zones. On the basis of chemical zoning of Na-pyroxene and garnet, Enami et al. (1994) and Enami (1998) indicated different P - T paths for each mineral zone; that is, a higher geothermal gradient for a higher metamorphic grade. However, assuming several P - T paths for the calculation makes it difficult to consider overall trends in the change of mineral parageneses. In this study, a specific P - T path was, therefore, assumed, as shown in Figure 1c, which covers peak P - T conditions from the chlorite zone to the oligoclase–biotite zone, cross-cutting the greenschist, blueschist, epidote–amphibolite and amphibolite facies.

4 | RESULTS

4.1 | Multivariate statistical analyses

k -means cluster analysis was performed for the CLR transformed and whitened data sets assuming five clusters (C1–C5). Results are shown in Figures 3a and 4, while Figure 5 shows the centroid of the KCA result. To reduce the data dimension, PCs were also calculated to produce a compositional biplot. The compositional biplot (Figure 3a and details of PCs are shown in Figure 3c,d) indicates both the data variability and relationship between variables (Aitchison & Greenacre, 2002). Vertices in close relations indicate that the ratios of these elements are almost

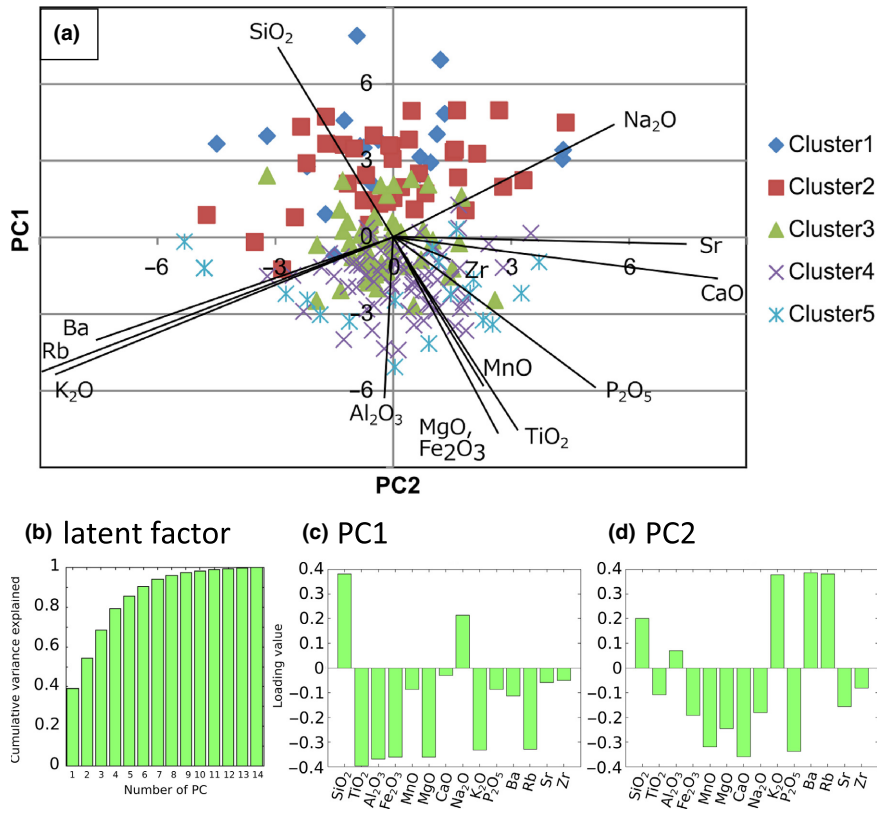


FIGURE 3 (a) Compositional biplot showing KCA results. PC loadings for each element are also plotted as black lines. Vertices in close relations indicate that the ratios of these elements are almost constant. Boundaries between clusters show the correlation with PC1. (b) Latent factor of PCA. (c, d) PC loadings of PC1 and PC2

constant (e.g. MgO, MnO, TiO₂ and Fe₂O₃) (Figure 3a). Figure 3b shows the cumulative latent factors calculated based on the Eigen values. These values indicate the variance accounted by each PC, that is, 54% of compositional variance can be explained by the first two PCs (PC1 and PC2). The details of these two PCs are shown in Figure 3c,d. Although attribution of PC1 and PC2 is not strongly dominant, these PCs represent the most and second intense characteristics of the data set, respectively. PC1 is characterized by a negative correlation between Si+Na and other elements (Figure 3c), and PC2 is characterized by a decoupling of Si, K, Ba and Rb from other components such as Fe and Mg (Figure 3d). KCA results for standardized and whitened data set would essentially correspond not to PCA but ICA (Iwamori et al., 2017); however, present KCA results seem to be well correlated to PC1, while PC2 shows almost no relationship (Figure 3a). This means that most dominant characteristic of the investigated data set can be consistently extracted by both PCA and ICA, which exhibits clusters that become poor in Si and Na with ascending order of the cluster as shown in Figure 4. The compositional variation of the clusters is also shown in Figure 5. Among the clusters, C5 is the most CaO-rich and MgO-rich composition and C1 is the most MnO-rich one.

The spatial distribution of the clusters is shown in Figure 6a,b. Significant relationships between clusters and metamorphic grade are apparent. The observed trends seem

to be different in the eastern and western areas. In the western area (Figure 6a,c), the high-grade metamorphic rocks (oligoclase–biotite and albite–biotite zones) are dominated by C4 and C5, while C1–C3 are observed mainly in the lower-grade region (garnet and chlorite zones). This relationship is also indicated in Figure 6c showing the increase trend of C4 and C5 with the metamorphic grade in the western part. In contrast, C5 is rare in the eastern area, while C4 becomes dominant in the albite- and oligoclase–biotite zone (Figure 6).

Negative matrix factorization analyses indicate four independent end-members of whole-rock composition (X1–X4). The areal distribution of the NMF result is shown in Figure 7, and details of end-member compositions are listed in Table 1. These four end-members have varying SiO₂ contents, indicating that SiO₂ increase/decrease is correlated with increase/decrease of some specific elements of the studied data set. X3 is the most SiO₂-rich component among the obtained end-members, and all samples contain significant amount of X3 component with the average of 81%. The remaining ~20% is accounted for by variable amounts of the other three end-members. These variations are systematically different between the western and eastern part (Figure 7). Tetrahedral plots of the NMF results for the western and eastern areas are shown in Figure 8a,b, respectively, where metamorphic grades are indicated by colour. A bar plot showing the proportions of each end-member component in respective metamorphic zones is also shown in Figure 8c. This

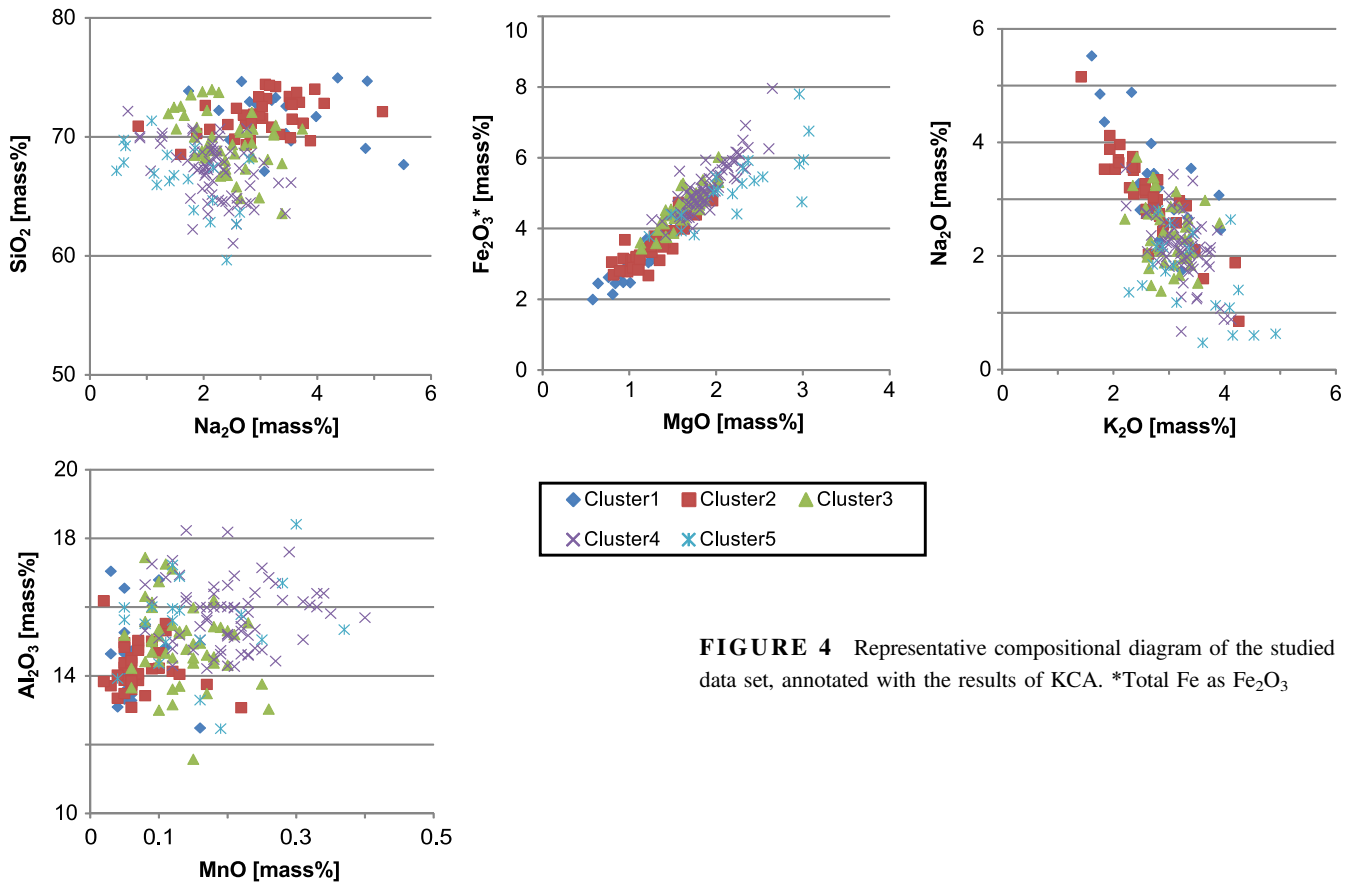


FIGURE 4 Representative compositional diagram of the studied data set, annotated with the results of KCA. *Total Fe as Fe_2O_3

figure shows, for example, ~30% of the samples in the oligoclase–biotite zone in the western part contain <5% of X1 component. Therefore, increase of red (0%–5% occupancy) or green (5%–10%) colour compared to purple (10%–15%) or blue (15%–20%) in this figure (such as X1, X2 and X4 components) indicates the increase of the samples poor in these components, in other words, decrease of the relevant components. In the western area, a clear compositional trend is apparent from the chlorite zone to the oligoclase–biotite zone, with the increase of X2

component and compensating decrease of X4 component with metamorphic grade. As the X2 component contains significant amounts of Ca, Fe and Mg, and X4 component contains Si and Na, this evolutionary change indicates increase in Ca, Fe and Mg, and slight decreases in Na and Si. In contrast, samples from the eastern area show a much weaker trend with slight increase of X2 component and decrease of X1 and X4 components.

4.2 | Thermodynamic modelling

Whole-rock composition changes continuously from X2-poor low-grade samples to X2-rich high-grade samples. Representative compositions for low- and high-grade samples were defined by the averages of the chlorite zone and oligoclase–biotite zone samples in the western part, respectively (Table 2). A $P(T)$ – X equilibrium phase diagram was constructed for these representative low- and high-grade whole-rock compositions (Figure 9). Since whole-rock compositions of the eastern area are widely scattered, only samples from the western area were used. The stability field for the biotite-absent assemblage was observed in the low-grade compositions at <500°C, and in the medium- to high-grade compositions at <310°C. Garnet is stable under 310°C. The calculated order of index minerals is concordant with the order of the chlorite, garnet and biotite zones.

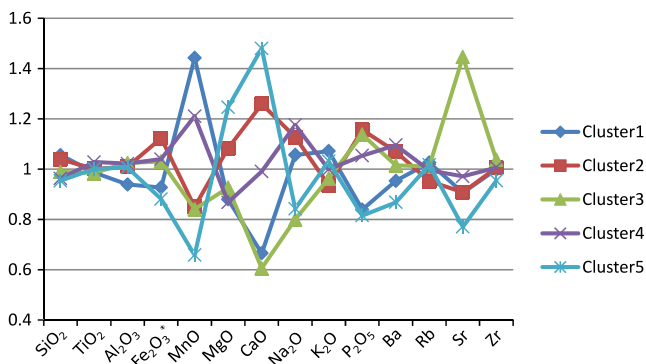


FIGURE 5 Centroids obtained by cluster analysis (KCA). Each element is normalized to the mean of the centroids, which are obtained from the iterative calculation of the k-means clustering algorithm

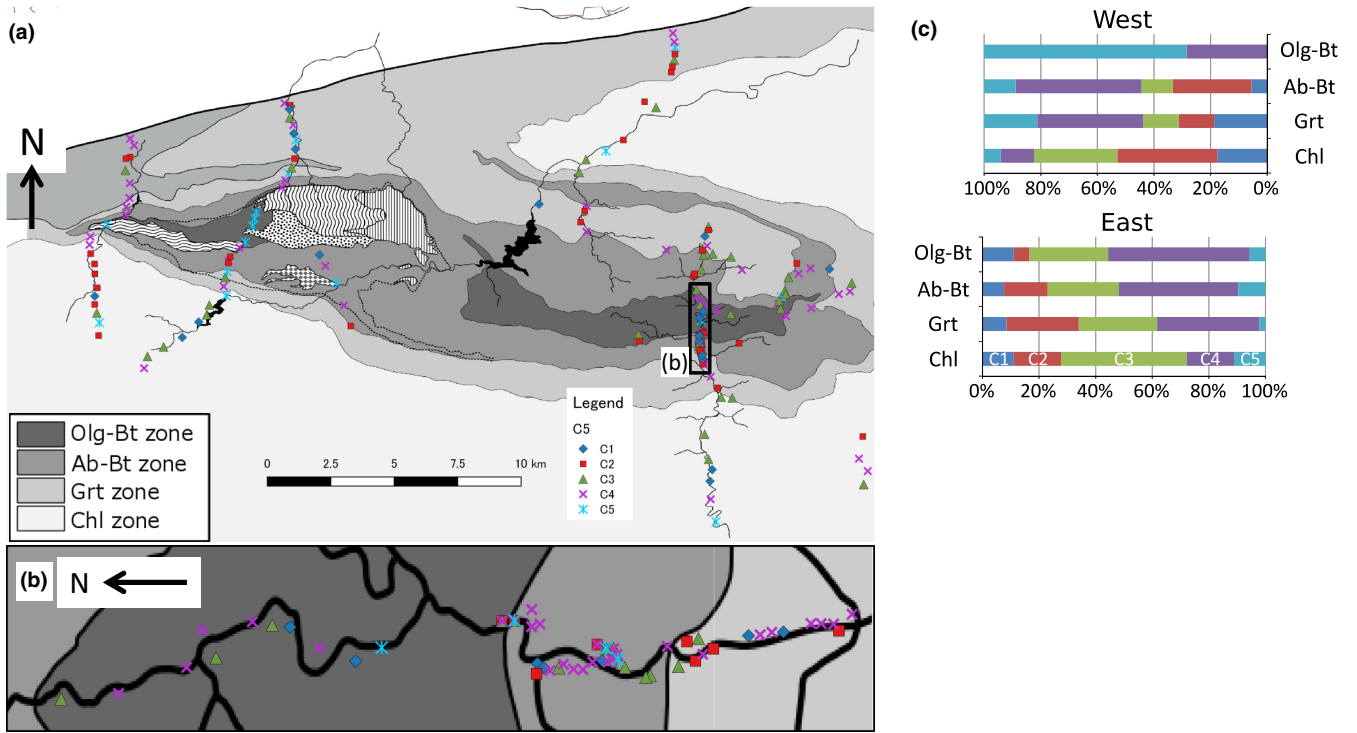


FIGURE 6 (a) Areal distribution of KCA ($C = 5$). In the high-grade zones (oligoclase- and albite–biotite zones) of the western area, C4 and C5 are the dominant clusters, whereas the compositional trend is less obvious in the eastern area. Zonal metamorphic map is after Higashino (1990). Dotted line indicates the boundary of the proposed eclogite nappe (Aoya et al., 2013). (b) Closed view of the rectangle area in the eastern part. (c) Proportion of each cluster in the respective metamorphic zones with respect to the western/eastern parts

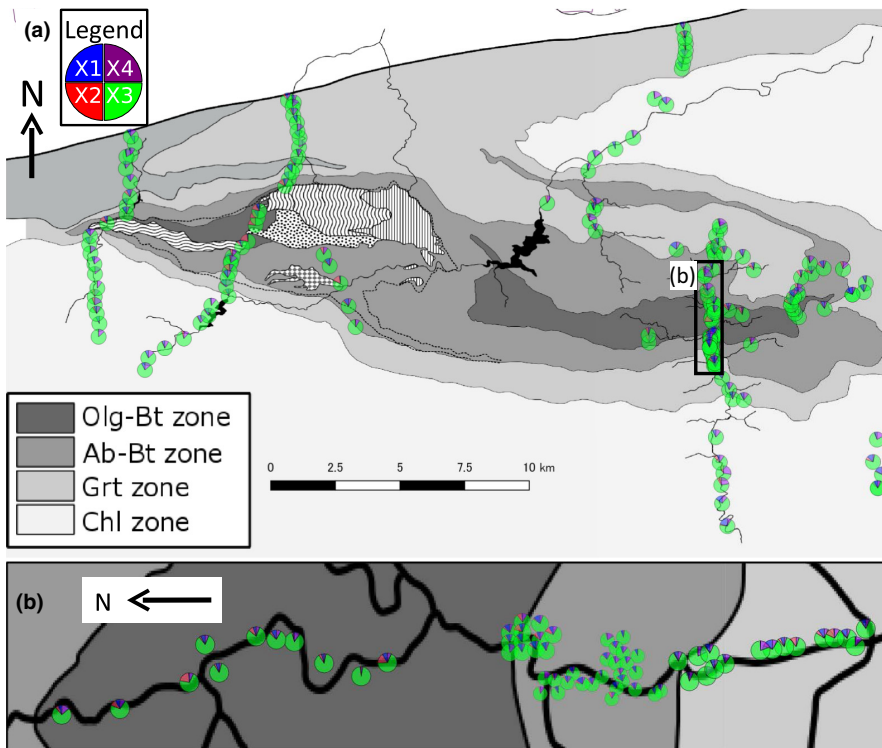


FIGURE 7 (a) Areal distribution of NMF results in central Shikoku. In the western area, high-grade zone is occupied by X2-rich samples, whereas the eastern area does not show an obvious trend. (b) Enlarged view of the eastern area marked by a black rectangle in (a). X2 (red colour) is less obvious in the eastern area

At the conditions of the chlorite zone, K-feldspar is stable ($<310^{\circ}\text{C}$), which is rarely reported in the natural observation of the Sanbagawa metamorphic belt. However, the

volume fraction of the calculated K-feldspar is small (<2 vol.% at 300°C and low-grade composition), and this misfit may be negligible. Under conditions of the

TABLE 1 Calculated end-members of NMF

	X1	X2	X3	X4
SiO ₂	16.2	40.5	76.5	63.5
TiO ₂	0.7	1.1	0.5	0.4
Al ₂ O ₃	32.3	19.0	14.5	12.4
FeO ^a	25.5	10.8	2.5	3.8
MnO	1.0	0.3	0.1	0.0
MgO	11.8	5.5	0.8	2.1
CaO	0.0	15.8	0.5	0.1
Na ₂ O	0.7	3.8	1.3	16.4
K ₂ O	8.8	1.7	3.0	0.8
P ₂ O ₅ ^b	0.2	0.3	0.1	0.1
Ba ^b	0.093	0.013	0.052	0.005
Rb ^b	0.054	0.015	0.009	0.014
Si ^b	0.006	0.111	0.008	0.023
Zr ^b	0.032	0.025	0.011	0.033
Total	97.0	98.4	99.6	99.5
O=		13.9		
Si		3.62		
Ti		0.08		
Al		2.00		
Fe ²⁺		0.81		
Mn		0.02		
Mg		0.74		
Ca		1.52		
Na		0.66		
K		0.20		
Σ(M ²⁺) ^c		3.08		

Stoichiometry of X2 is calculated on the basis of Al = 2.

^aAll iron values are calculated as FeO.

^bNot included in the total.

^cSum of Fe²⁺, Mn, Mg and Ca.

oligoclase–biotite zone (600°C and 1 GPa), the stable mineral assemblages are phengite, garnet, plagioclase, biotite, quartz and rutile±paragonite for low-grade compositions and phengite, garnet, plagioclase, biotite, epidote, quartz and rutile±amphibole for high-grade compositions. The occurrence of sub-calcic amphibole is reported in the high-grade zone of the Sanbagawa belt (e.g. Aoya et al., 2013; Goto et al., 1996), and thus, this high-grade mineral assemblage is concordant with those observed in natural samples. Conversely, low-grade compositions stabilize paragonite as a sodic phase, which is also inferred as a high-*P* stable phase in the metapelites in the Sanbagawa belt (e.g. Kouketsu, Enami, Mouri, Okamura, & Sakurai, 2014). The whole-rock H₂O content (stored as mineral-bound water) and modal amount of garnet were also calculated as shown in Figure 9b, which indicates that H₂O content and modal

garnet vary with whole-rock composition, ranging from low at low-grade compositions to high at high-grade compositions.

5 | DISCUSSION

5.1 | Evolutional change of the whole-rock composition

Both KCA and NMF results indicate systematic compositional changes in the analysed data set. The areal distribution of the clusters (Figure 6) indicates that the eastern and western areas have different compositional trends, with the western area having a clearer trend than the eastern area. Samples of the most SiO₂-poor and Ca-rich cluster (C5; Figure 5) are observed in the oligoclase–biotite zone of the western area. Monotonous increase of C4 is also recognized from the chlorite to albite–biotite zones. A similar trend is observed in the eastern area, although the dominance of C5 is not observed among the oligoclase–biotite zone. NMF results show that samples in the oligoclase–biotite zone of the western area are rich in the X2 component (i.e. rich in Ca, Mg and Fe), while samples in the oligoclase–biotite zone of the eastern area show relatively similar but more widely scattered compositions. These results indicate a systematic difference in the whole-rock composition between the western and eastern areas. In the western area, large eclogitic mafic bodies are observed (e.g. Aoya, 2001; Takasu, 1984), whereas no significant eclogitic mafic body has been recognized in the eastern area (although there are some mafic layers, some of which have been recently assigned to the eclogite facies; e.g. Taguchi & Enami, 2014; Uno, Iwamori, & Toriumi, 2015). Recent studies have proposed that the eclogitic bodies and surrounding pelitic schists in the western area once formed a continuous eclogite nappe (e.g. Aoya et al., 2013; Kouketsu et al., 2014). According to this idea, a large portion of the oligoclase–biotite and albite–biotite zone of the western area would have been subducted to conditions of the eclogite facies prior to the main Sanbagawa metamorphism, and have suffered higher pressure metamorphism than previously estimated for the oligoclase–biotite zone. The regional differences between the western and eastern areas can be related in part to the different settings of protolith generation or large-scale deformation structures, especially, high abundance of C5 near the large mafic bodies in the western part might be attributed to the mechanical mixing or chemical reactions brought from them.

However, despite regional differences in whole-rock compositions, we can see a monotonous change in whole-rock composition related to the metamorphic degree. For example, change in the proportion of clusters among the chlorite to albite–biotite zones, and the albite–biotite to

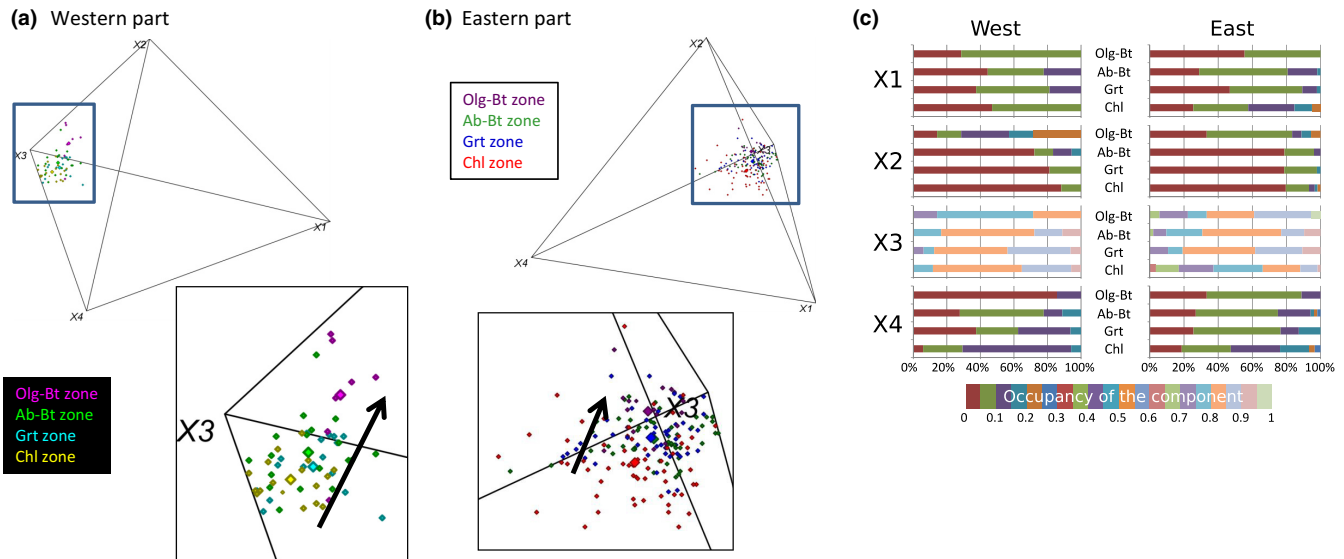


FIGURE 8 (a, b) Tetrahedral plot of NMF components. Rectangle areas are enlarged view. (a) and (b) show the western and eastern areas, respectively. Large diamonds show the mean values for each metamorphic grade. (c) Bar plots showing the proportion of the occupancy of each component in the samples of respective mineral zones. Occupancy of the component increases with the order of red, green, purple, etc., with 5% steps. For example, ~30% of the samples in the oligoclase–biotite zone in the western part have less than 5% of X1 component

TABLE 2 End-member composition for the pseudosection modelling shown in Figure 9

	X = 0	X = 1
SiO ₂	72.07	67.91
TiO ₂	0.55	0.63
Al ₂ O ₃	15.03	16.04
FeO ^a	4.03	5.43
MnO	0.12	0.16
MgO	1.44	2.08
CaO	0.65	2.40
Na ₂ O	2.98	2.04
K ₂ O	2.95	3.10
Total	99.82	99.78

^aAll iron values are calculated as FeO.

oligoclase–biotite zones in the western area (Figure 6c). Since each mineral zone has an independent prograde P – T path, changes from the low-grade chlorite zone to high-grade oligoclase–biotite zone do not directly show the evolutionary change that occurred in the palaeo-subduction zone; however, we can deduce the evolution of metapelite whole-rock chemistry with increasing metamorphic grade from these results. The higher-grade samples are more likely classified as either C4 or C5 and the lower-grade samples as C1 or C2. Higher-grade samples, thus, tend to be poor in SiO₂ and Na₂O, and rich in MgO, FeO, TiO₂, MnO and Al₂O₃.

The NMF results show a similar trend, especially in the western area. As shown in Figure 7, samples collected from the albite–biotite and oligoclase–biotite zones are

richer in the X2 component which is rich in FeO and MgO. In the eastern area, enrichment of the X2 component is not as significant, most likely due to the wide variety of the chlorite zone samples. The X2 component in the eastern part is slightly higher in the oligoclase–biotite zone. Furthermore, decrease of X4 component can be recognized in the lower-grade zones (Figure 8c). Decrease of X4 component corresponds to decrease of Na₂O and SiO₂ which is also observed in the western part.

These progressive changes are recognized in both western and eastern parts, in spite of the existence of eclogite nappe that could cause the difference in protolith compositions. This fact indicates that the protoliths of the studied area may have been fairly similar.

Progressive change in whole-rock compositions has previously been discussed only for trace elements, especially trace element ratios (e.g. Bebout, Bebout, & Graham, 2007; Bebout, Ryan, Leeman, & Bebout, 1999), because the absolute concentration of major elements can vary from sample to sample. On the basis of published whole-rock analyses including those of Goto et al. (1996), Enami (1998) concluded that there is no systematic change in whole-rock composition, at least between the garnet and albite–biotite zones. Our results suggest, however, that there is a systematic change in whole-rock composition with metamorphic grade (Figure 8a,b).

Compositional trends with progressive metamorphism can be expressed by the increasing X2 component, which closely resembles garnet. Though the X2 composition has excess Si, Na and K, if its stoichiometric formula is calculated by setting Al = 2, then Si, Al and $\Sigma(\text{Fe}+\text{Mn}+\text{Mg}+\text{Ca})$

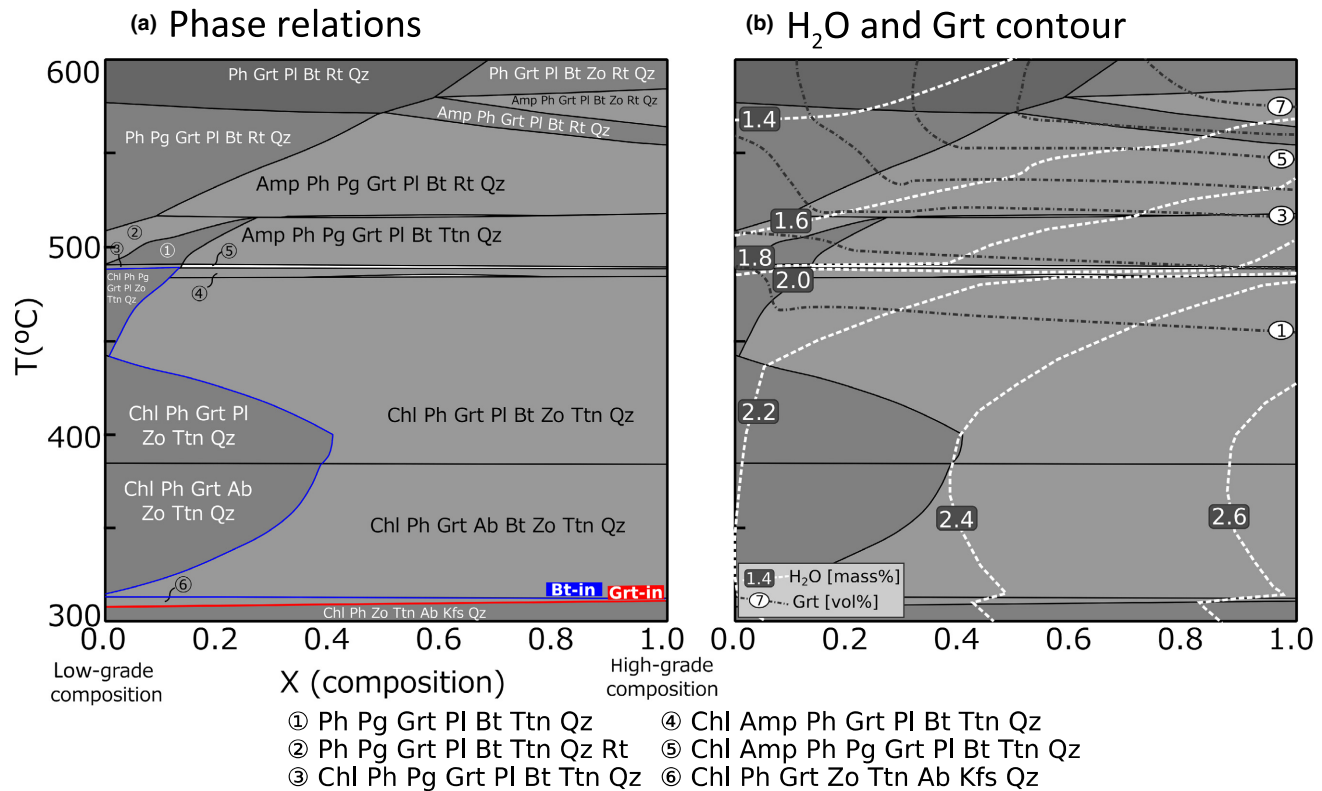
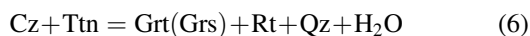
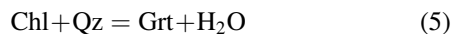


FIGURE 9 $P(T)$ - X diagram calculated for a representative subduction P - T trajectory of the Sanbagawa metamorphic belt. The P - T relationship used in the calculation is shown in Figure 1c. (a) Stable phase relations. P - T -bulk path will start from the left-bottom and go to right-top. Biotite and garnet in line are shown in blue and red colours, respectively. (b) Contours show the water content bound in solid phases and calculated amount of modal garnet

have the ratio of 3.6:2:3 which is similar to that of garnet (Table 1). This can be attributed to the “precipitation” of garnet and effusion of other components during progressive metamorphism. This is also indicated by Figure 9b, as the modal amount of garnet is higher in the high-grade whole-rock composition under the same P - T conditions. Given that garnet is stable over a wide range of P - T , once it is crystallized, decomposition is unlikely to occur during the prograde stage. Several garnet-forming reactions have been proposed for the prograde metamorphism of the Sanbagawa metamorphic belt (e.g. Banno, Sakai, & Higashino, 1986; Enami, 1998; Yoshida & Hirajima, 2015); for example:



During the progress of these reactions, a considerable amount of aqueous fluid would be released from the rock system. Aqueous fluid that exists under increasing P - T can dissolve and transport a variety of components (Hermann, Spandler, Hack, & Korsakov, 2006; Kessel, Schmidt, Ulmer, & Pettke, 2005; Putnis & John, 2010; Uno et al., 2014). Dehydration reactions during progressive

metamorphism could, therefore, be a possible cause of the change in whole-rock composition. PCA results indicate that Si and Na have negative correlation with other components. On the basis of natural fluid inclusions, Yoshida et al. (2015) indicated the existence of NaCl-rich aqueous fluid (~10 mass%) near peak P - T conditions of the high-grade rocks (albite-biotite and oligoclase-biotite zones) of the studied area, which could transport a certain amount of albite as a dissolved component (e.g. Shmulovich, Graham, & Yardley, 2001). Therefore, the enrichment of the garnet (X2) component may be attributed to the removal of the albite component by aqueous fluids, although fixing of garnet is less obvious in the eastern part.

Scattered data trend observed in the eastern area may be partly explained by severe fluid activities during exhumation, as many deformation structures and fluid-related veins are observed (e.g. Uno et al., 2015; Yoshida et al., 2015). Fluid infiltration during exhumation of the metamorphic belt may explain the scattered compositional data in the eastern area (Figure 8b). On the basis of concentration of fluid-immobile element and LOI values, Uno et al. (2014) indicated that a certain amount of the hornblende component has been transferred with pervasive fluid flow during the exhumation stage

of the high-grade zone of the eastern area. There is a possibility that such fluid activity affected the compositional evolution of the studied metamorphic rocks.

5.2 | Water stored in the solid phase

Thermodynamic calculations predict different mineral assemblages for low- and high-grade compositions (Figure 9). If the subducted material follows the evolutionary change of whole-rock composition from the low- to high-grade compositions with increasing P - T , the observed mineral assemblage would change from chlorite-bearing/garnet-biotite-absent, through chlorite-garnet-bearing/biotite-absent, to garnet-biotite-bearing assemblages, which correlates well with the metamorphic zonation of the Sanbagawa metamorphic belt. Matsumoto, Banno, and Hirajima (2005) indicated that the 0.1–0.2 mass% of MnO in the metapelitic rocks would considerably extend the stability field of garnet towards lower temperatures. The MnO content of the whole-rock composition used for the calculation is almost the same as the value of 0.15 mass%, and thus, garnet becomes stable at the low- T conditions such as 310°C.

Figure 9b indicates that high-grade samples can retain more water at given P - T conditions than low-grade samples. The dehydration process under conditions of the greenschist facies (~350–450°C) is driven mainly by the breakdown of chlorite, which is an important water reservoir in low- T metamorphism (e.g. Kuwatani, Okamoto, & Toriumi, 2011; Sato, Hirajima, Yoshida, Kamimura, & Fujimoto, 2016). Kuwatani et al. (2011) performed thermodynamic forward modelling of the dehydration process for mafic rocks, revealing that the water content of mafic rocks was controlled mainly by the modal amount of chlorite under greenschist facies conditions. If the P - T path is cold, dehydrated aqueous fluid would be buffered by growth of other hydrous phases such as lawsonite (Sato et al., 2016), whereas a warm P - T path causes a significant decrease in bulk H₂O content (Kuwatani et al., 2011). However, H₂O contours (Figure 9b) indicate that changes from low- to high-grade whole-rock compositions correspond to increasing whole-rock H₂O content, although increasing P - T itself causes some dehydration. Therefore, evolutionary changes in whole-rock compositions would suppress dehydration during progressive metamorphism. This effect should be considered in forward modelling of considering the fluid cycle in subduction zones, although a quantitative model has not yet been established.

ACKNOWLEDGEMENTS

This work was partly supported by JSPS KAKENHI grants nos JP16K17835 for K.Y., JP25257208 for T.H.,

4503 (no. JP2512005 for T.K. and no. JP25120011 for S.A.), and JP15K20864 for T.K. Financial support was also provided by JST PRESTO (grant no. JPMJPR1676) for T.K. Members of the Joint Usage/Research Center programme no. 2015-B-04 from the Earthquake Research Institute, University of Tokyo, are thanked for fruitful discussions. This article benefited from constructive reviews by Y. Kouketsu and K. Miyazaki and editorial handling by K. Evans.

ORCID

Kenta Yoshida  <http://orcid.org/0000-0001-9525-1598>

REFERENCES

- Aggarwal, C. C., & Zhai, C.X., eds. (2012). *Mining text data*. New York: Springer Science & Business Media.
- Aitchison, J. (1986). *The statistical analysis of compositional data*. London: Chapman and Hall, 416 pp.
- Aitchison, J., & Greenacre, M. (2002). Biplots of compositional data. *Journal of the Royal Statistical Society: Series C (Applied Statistics)*, 51, 375–392.
- Aoya, M. (2001). P - T - D path of eclogite from the Sambagawa belt deduced from combination of petrological and microstructural analyses. *Journal of Petrology*, 42, 1225–1248.
- Aoya, M., Noda, A., Mizuno, K., Mizukami, T., Miyachi, Y., Matsuura, H., . . . Aoki, M. (2013). Geology of the Niihama District. Quadrangle Series, 1:50,000, Geological Survey of Japan, AIST. 181 pp.
- Audetát, A., & Keppler, H. (2005). Solubility of rutile in subduction zone fluids, as determined by experiments in the hydrothermal diamond anvil cell. *Earth and Planetary Science Letters*, 232, 393–402.
- Auzanneau, E., Schmidt, M. W., Vielzeuf, D., & Connolly, J. D. (2010). Titanium in phengite: A geobarometer for high temperature eclogites. *Contributions to Mineralogy and Petrology*, 159, 1–24.
- Banno, S. (2004). Brief history of petro-tectonic research of the Sanbagawa Belt, Japan. *The Island Arc*, 13, 475–483.
- Banno, S., Sakai, C., & Higashino, T. (1986). Pressure-temperature trajectory of the Sanbagawa metamorphism deduced from garnet zoning. *Lithos*, 19, 51–63.
- Batchelor, R. A., & Bowden, P. (1985). Petrogenetic interpretation of granitoids rock series using multicationic parameters. *Chemical Geology*, 48, 43–55.
- Bebout, G. E., Bebout, A. E., & Graham, C. M. (2007). Cycling of B, Li, and LILE (K, Cs, Rb, Ba, Sr) into subduction zones: SIMS evidence from micas in high- P/T metasedimentary rocks. *Chemical Geology*, 239, 284–304.
- Bebout, G., Ryan, J. G., & Leeman, W. P. (1993). B-Be systematics in subduction-related metamorphic rocks: Characterization of the subducted component. *Geochimica et Cosmochimica Acta*, 57, 2227–2237.
- Bebout, G. E., Ryan, J. G., Leeman, W. P., & Bebout, A. E. (1999). Fractionation of trace elements by subduction-zone metamorphism – Effect of convergent-margin thermal evolution. *Earth and Planetary Science Letters*, 171, 63–81.

- Blei, D. M., Ng, A. Y., & Jordan, M. I. (2003). Latent dirichlet allocation. *Journal of Machine Learning Research*, 3, 993–1022.
- Brandmeier, M., & Wörner, G. (2016). Compositional variations of ignimbrite magmas in the Central Andes over the past 26 Ma – A multivariate statistical perspective. *Lithos*, 262, 713–728.
- Bucher-Nurminen, K., Frank, E., & Frey, M. (1983). A model for the progressive regional metamorphism of margarite-bearing rocks in the Central Alps. *American Journal of Science*, 283, 370–395.
- Coggon, R., & Holland, T. J. B. (2002). Mixing properties of phengitic micas and revised garnet–phengite thermobarometers. *Journal of Metamorphic Geology*, 20, 683–696.
- Connolly, J. A. D. (2005). Computation of phase equilibria by linear programming: A tool for geodynamic modeling and its application to subduction zone decarbonation. *Earth and Planetary Science Letters*, 236, 524–541.
- Dale, J., Powell, R., White, R. W., Elmer, F. L., & Holland, T. J. B. (2005). A thermodynamic model for Ca–Na clin amphiboles in Na₂O–CaO–FeO–MgO–Al₂O₃–SiO₂–H₂O–O for petrological calculations. *Journal of Metamorphic Geology*, 23, 771–791.
- Enami, M. (1982). Oligoclase–biotite zone of the Sanbagawa metamorphic terrain in the Bessi district, central Shikoku, Japan. *Journal of the Geological Society of Japan*, 88, 887–900.
- Enami, M. (1998). Pressure–temperature path of Sanbagawa prograde metamorphism deduced from grossular zoning of garnet. *Journal of Metamorphic Geology*, 16, 97–106.
- Enami, M., Wallis, S. R., & Banno, Y. (1994). Paragenesis of sodic pyroxene-bearing quartz schists: Implications for the P–T history of the Sanbagawa belt. *Contributions to Mineralogy and Petrology*, 116, 128–198.
- Endo, S. (2010). Pressure–temperature history of titanite-bearing eclogite from the Western Iratsu body, Sanbagawa Metamorphic Belt, Japan. *Island Arc*, 19, 313–335.
- Endo, S., Wallis, S. R., Hirata, T., Anczkiewicz, R., Platt, J., Thirlwall, M., & Asahara, Y. (2009). Age and early metamorphic history of the Sanbagawa belt: Lu–Hf and P–T constraints from the Western Iratsu eclogite. *Journal of Metamorphic Geology*, 27, 371–384.
- Endo, S., Wallis, S. R., Tsuboi, M., Aoya, M., & Uehara, S. (2012). Slow subduction and buoyant exhumation of the Sanbagawa eclogite. *Lithos*, 146–147, 183–201.
- Evans, T. P. (2004). A method for calculating effective bulk composition modification due to crystal fractionation in garnet-bearing schist: Implications for isopleth thermobarometry. *Journal of Metamorphic Geology*, 22, 547–557.
- Frank, E. (1983). Alpine metamorphism of calcareous rocks along a cross-section in the Central Alps: Occurrence and breakdown of muscovite, margarite and paragonite. *Schweizerische Mineralogische und Petrographische Mitteilungen*, 63, 37–93.
- Goto, A., Higashino, T., & Sakai, C. (1996). XRF analyses of Sanbagawa pelitic schists in central Shikoku, Japan. *Memoirs of Faculty of Science, Kyoto University, Series of Geology and Mineralogy*, 58, 1–19.
- Hermann, J., Spandler, C., Hack, A., & Korsakov, A. V. (2006). Aqueous fluids and hydrous melts in high-pressure and ultra-high pressure rocks: Implications for element transfer in subduction zones. *Lithos*, 92, 399–417.
- Higashino, T. (1990). The higher grade metamorphic zonation of the Sambagawa metamorphic belt in central Shikoku, Japan. *Journal of Metamorphic Geology*, 8, 413–423.
- Higashino, F., Kawakami, T., Tsuchiya, N., Satish-Kumar, M., Ishikawa, M., Grantham, G. H., . . . Hirata, T. (2015). Geochemical behavior of zirconium during Cl-rich fluid or melt infiltration under upper amphibolite facies metamorphism — A case study from Brattnipene, Sør Rondane Mountains, East Antarctica. *Journal of Mineralogical and Petrological Sciences*, 110, 166–178.
- Holland, T. J. B., & Powell, R. (1998). An internally consistent thermodynamic data set for phases of petrological interest. *Journal of Metamorphic Geology*, 16, 309–343.
- Igarashi, Y., Nagata, K., Kuwatani, T., Omori, T., Nakanishi-Ohno, Y., & Okada, M. (2016). Three levels of data-driven science. *Journal of Physics: Conference Series*, 699, 012001.
- Iwamori, H., Yoshida, K., Nakamura, H., Kuwatani, T., Hamada, M., Haraguchi, S., & Ueki, K. (2017). Classification of geochemical data based on multivariate statistical analyses: Complementary roles of cluster, principal component, and independent component analyses. *Geochemistry, Geophysics, Geosystems*, 18, 994–1012. <https://doi.org/10.1002/2016GC006663>
- John, T., Gussone, N., Podladchikov, Y. Y., Bebout, G. E., Dohmen, R., Halam, R., . . . Seitz, H.-M. (2012). Volcanic arcs fed by rapid pulsed fluid flow through subducting slabs. *Nature Geoscience*, 5, 489–492.
- Kessel, R., Schmidt, M. W., Ulmer, P., & Pettke, T. (2005). Trace element signature of subduction-zone fluids, melts and supercritical liquids at 120–180 km depth. *Nature*, 437, 724–727.
- Kiminami, K., & Ishihama, S. (2003). The percentage of low-grade metasediments in the Sanbagawa Metamorphic Belt, Shikoku, southwest Japan, based on whole-rock geochemistry. *Sedimentary Geology*, 159, 257–274.
- Konrad–Schmolke, M., O’Brien, P. J., & Zack, T. (2011). Fluid migration above a subducted slab—constraints on amount, pathways and major element mobility from partially overprinted eclogite-facies rocks (Sesia Zone, Western Alps). *Journal of Petrology*, 52, 457–486.
- Kouketsu, T., & Enami, M. (2011). Calculated stabilities of sodic phases in the Sambagawa metapelites and their implications. *Journal of Metamorphic Geology*, 29, 301–316.
- Kouketsu, Y., Enami, M., Mouri, T., Okamura, M., & Sakurai, T. (2014). Composite metamorphic history recorded in garnet porphyroblasts of Sambagawa metasediments in the Besshi region, central Shikoku, Southwest Japan. *Island Arc*, 23, 263–280.
- Kurata, H., & Banno, S. (1974). Low-grade progressive metamorphism of pelitic schists of the Sazare area, Sanbagawa metamorphic terrain in central Shikoku, Japan. *Journal of Petrology*, 15, 361–382.
- Kuwatani, T., Okamoto, A., & Toriumi, M. (2011). Thermodynamic forward modeling of progressive dehydration reactions during subduction of oceanic crust under greenschist facies conditions. *Earth and Planetary Science Letters*, 307, 9–18.
- Maier, W. D., Arndt, N. T., & Curl, E. A. (2000). Progressive crustal contamination of the Bushveld Complex: Evidence from Nd isotopic analyses of the cumulate rocks. *Contributions to Mineralogy and Petrology*, 140, 316–327.
- Matsumoto, K., Banno, S., & Hirajima, T. (2005). Pseudosection analysis for the Sanbagawa pelitic schist and its implication to the thermal structure of high-pressure intermediate type of metamorphism. *Proceedings of the Japan Academy, Series B*, 81, 273–277.
- Miyagi, Y., & Takasu, A. (2005). Prograde eclogites from the Tonaru epidote amphibolite mass in the Sambagawa Metamorphic Belt, central Shikoku, southwest Japan. *Island Arc*, 14, 215–235.

- Ohta, T., & Arai, H. (2006). Problems in compositional data analysis and their solutions. *Journal of the Geological Society of Japan*, 112, 173–187.
- Okudaira, T., Shigematsu, N., Harigane, Y., & Yoshida, K. (2017). Grain size reduction due to fracturing and subsequent grain-size-sensitive creep in a lower crustal shear zone in the presence of a CO₂-bearing fluid. *Journal of Structural Geology*, 95, 171–187.
- Pawłowsky-Glahn, V., & Egozcue, J. J. (2006). Compositional data and their analysis: An introduction. *Geological Society, London, Special Publications*, 264, 1–10.
- Putnis, A., & John, T. (2010). Replacement processes in the Earth's crust. *Elements*, 6, 159–164.
- Sato, E., Hirajima, T., Yoshida, K., Kamimura, K., & Fujimoto, Y. (2016). Phase relations of lawsonite-blueschists and their role as a water-budget monitor: A case study from the Hakoishi sub-unit of the Kurosegawa belt, SW Japan. *European Journal of Mineralogy*, 28, 1029–1046.
- Shmulovich, K., Graham, C., & Yardley, B. (2001). Quartz, albite and diopside solubilities in H₂O-NaCl and H₂O-CO₂ fluids at 0.5–0.9 GPa. *Contributions to Mineralogy and Petrology*, 141, 95–108.
- Spandler, C., Hermann, J., Arculus, R., & Mavrogenes, J. (2003). Redistribution of trace elements during prograde metamorphism from lawsonite blueschist to eclogite facies; implications for deep subduction-zone processes. *Contributions to Mineralogy and Petrology*, 146, 205–222.
- Taguchi, T., & Enami, M. (2014). Coexistence of jadeite and quartz in garnet of the Sanbagawa metapelite from the Asemi-gawa region, central Shikoku, Japan. *Journal of Mineralogical and Petrological Sciences*, 109, 169–174.
- Takasu, A. (1984). Prograde and retrograde eclogites in the Samba-gawa metamorphic belt, Besshi district, Japan. *Journal of Petrology*, 25, 619–643.
- Thompson, J. B. (1957). The graphical analysis of mineral assemblages in pelitic schists. *The American Mineralogist*, 42, 842–858.
- Tinkham, D. K., & Ghent, E. D. (2005). Estimating P-T conditions of garnet growth with isochemical phase-diagram sections and the problem of effective bulk-composition. *The Canadian Mineralogist*, 43, 35–50.
- Tolosana-Delgado, R., Otero, N., & Pawłowsky-Glahn, V. (2005). Some basic concepts of compositional geometry. *Mathematical Geology*, 37, 673–680.
- Tsuchiya, S., & Hirajima, T. (2013). Evidence of the lawsonite eclogite facies metamorphism from an epidote–glaucophane eclogite in the Kotsu area of the Sanbagawa belt, Japan. *Journal of Mineralogical and Petrological Sciences*, 108, 166–171.
- Uno, M., Iwamori, H., Nakamura, H., Yokokawa, T., Ishikawa, T., & Tanimizu, M. (2014). Elemental transport upon hydration of basic schists during regional metamorphism: Geochemical evidence from the Sanbagawa metamorphic belt, Japan. *Geochemical Journal*, 48, 29–49.
- Uno, M., Iwamori, H., & Toriumi, M. (2015). Transition from dehydration to hydration during exhumation of the Sanbagawa metamorphic belt, Japan, revealed by the continuous P-T path recorded in garnet and amphibole zoning. *Contributions to Mineralogy and Petrology*, 170, 33.
- Verma, S. P., Rivera-Gómez, M. A., Díaz-González, L., Pandarinath, K., Amezcua-Valdez, A., Rosales-Rivera, M., ... Armstrong-Altrin, J. S. (2017). Multidimensional classification of magma types for altered igneous rocks and application to their tectonomagmatic discrimination and igneous provenance of siliciclastic sediments. *Lithos*, 278–281, 321–330.
- Wallis, S. R., & Aoya, M. (2000). A re-evaluation of eclogite facies metamorphism in SW Japan: Proposal for an eclogite nappe. *Journal of Metamorphic Geology*, 18, 653–664.
- White, R. W., Powell, R., & Holland, T. J. B. (2001). Calculation of partial melting equilibria in the system Na₂O-CaO-K₂O-FeO-MgO-Al₂O₃-SiO₂-H₂O (NCKFMASH). *Journal of Metamorphic Geology*, 19, 139–153.
- White, R. W., Powell, R., Holland, T. J. B., & Worley, B. A. (2000). The effect of TiO₂ and Fe₂O₃ on metapelitic assemblages at greenschist and amphibolite facies conditions: Mineral equilibria calculations in the system K₂O-FeO-MgO-Al₂O₃-SiO₂-H₂O-TiO₂-Fe₂O₃. *Journal of Metamorphic Geology*, 18, 497–512.
- Whitney, D., & Evans, B. W. (2010). Abbreviations for names of rock-forming minerals. *American Mineralogist*, 95, 185–187.
- Yoshida, K., & Hirajima, T. (2015). 3D chemical mapping of 'Mn-caldera shaped zoning' garnet found from the Sanbagawa metamorphic belt of the Besshi district, SW Japan. *Journal of Mineralogical and Petrological Sciences*, 110, 197–213.
- Yoshida, K., Hirajima, T., Miyake, A., Tsuchiyama, A., Ohi, S., Nakano, T., & Uesugi, K. (2016). Combined FIB microsampling and X-ray microtomography: A powerful tool for the study of tiny fluid inclusions. *European Journal of Mineralogy*, 28, 245–256.
- Yoshida, K., Hirajima, T., Ohsawa, S., Kobayashi, T., Mishima, T., & Sengen, Y. (2015). Geochemical features and relative B-Li-Cl compositions of deep-origin fluids trapped in high-pressure metamorphic rocks. *Lithos*, 226, 50–64.

How to cite this article: Yoshida K, Kuwatani T, Hirajima T, Iwamori H, Akaho S. Progressive evolution of whole-rock composition during metamorphism revealed by multivariate statistical analyses. *J Metamorph Geol*. 2018;36:41–54. <https://doi.org/10.1111/jmg.12282>